

# Importance of Acid-Base Equilibrium in Electrocatalytic Oxidation of Formic Acid on Platinum

Jiyong Joo,<sup>†,‡</sup> Taro Uchida,<sup>‡</sup> Angel Cuesta,<sup>§</sup> Marc T. M. Koper,<sup>‡,#</sup> and Masatoshi Osawa<sup>\*,‡</sup>

<sup>†</sup> Graduate School of Chemical Sciences and Engineering, Hokkaido University, Sapporo 060-8682, Japan

<sup>‡</sup> Catalysis Research Center, Hokkaido University, Sapporo 001-0021, Japan

<sup>§</sup> Instituto de Química Física “Rocasolano”, CSIC, C. Serrano 119, E-28006 Madrid, Spain

<sup>#</sup> Leiden Institute of Chemistry, Leiden University, 2300 RA Leiden, The Netherlands

## Supporting Information Placeholder

---

**ABSTRACT:** Electro-oxidation of formic acid on Pt in acid is one of the most fundamental model reactions in electrocatalysis. However, its reaction mechanism is still a matter of strong debate. Two different mechanisms, bridge-bonded adsorbed formate mechanism and direct oxidation mechanism, have been proposed by assuming *a priori* that formic acid is the major reactant. Through systematic examination of the reaction over a wide pH range (0–12) by cyclic voltammetry and surface-enhanced infrared spectroscopy (SEIRAS), we will show that the formate ion is the major reactant over the whole pH range examined, even in strong acid. The performance of the reaction is maximal at a pH close to the  $pK_a$  of formic acid. The experimental results are reasonably explained by a new mechanism in which formate ion is directly oxidized via a weakly adsorbed formate precursor. The reaction serves as a generic example illustrating the importance of pH variation in catalytic proton-coupled electron transfer reactions.

---

Electrooxidation of formic acid (HCOOH) to  $CO_2$ , the reaction taking place at the anode of direct formic acid fuel cells, is one of the most fundamental model electrocatalytic reactions and has been investigated intensively over the last four decades mostly in acidic media.<sup>1–4</sup> It is generally accepted that HCOOH is oxidized via a dual pathway mechanism; a main pathway via a reactive intermediate and a pathway involving adsorbed CO ( $CO_{ads}$ ), a catalytic poison.  $CO_{ads}$  is oxidized to  $CO_2$  at high potentials. The pathway involving  $CO_{ads}$  has well been established in the 1980s, while the main pathway, non-CO pathway, is still matter of strong debate. Samjeské et al.<sup>5</sup> and others<sup>6,7</sup> proposed, on the basis of surface-enhanced infrared spectroscopy in an ATR geometry (ATR-SEIRAS)<sup>8</sup> and electrochemical measurements, that a formate species adsorbed on the electrode surface through its two O atoms (bridge-bonded formate) is the intermediate in the non-CO pathway and its decomposition to  $CO_2$  is the rate-determining step (bridge-bonded formate mechanism), while Chen et al.<sup>9</sup> argued that the adsorbed formate is a site-blocking spectator and that HCOOH is directly oxidized via a weakly adsorbed HCOOH precursor (direct HCOOH mechanism). A consensus has not been reached yet, either in theoretical studies of the reaction.<sup>10–12</sup> The aim of the present Communication is to make clear the real reaction mechanism through a systematic investigation of the reaction over a wide range of pH (0–12).

Since HCOOH is a weak acid with a  $pK_a$  of 3.75,<sup>13</sup> if the direct HCOOH pathway were the main reaction route, the oxidation current should decrease with increasing pH due to the decrease of HCOOH concentration. However, several earlier studies have reported that the oxidation current increases with pH.<sup>14</sup> Figure 1a shows representative cyclic voltammograms (CVs) for a rotating Pt disc electrode in 0.2 M

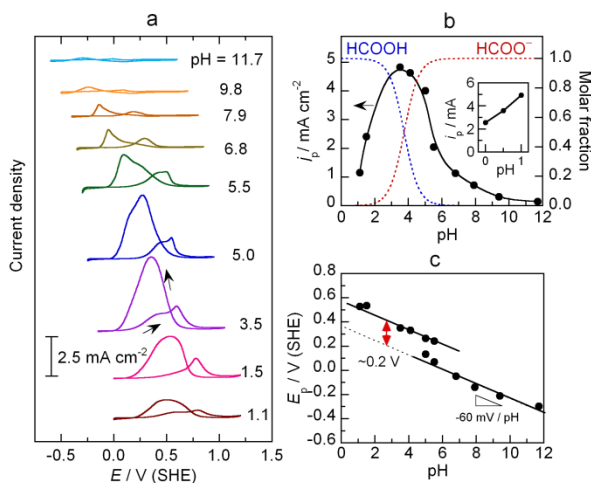


**Figure 1.** (a) Cyclic voltammograms of a rotating Pt disk electrode (1000 rpm) at  $50 \text{ mV s}^{-1}$  in 0.2 M phosphate buffer solutions or 0.5–1 M  $\text{H}_3\text{PO}_4$  (for  $\text{pH} < 2$ ) containing 50 mM  $\text{HCOONa}$ . (b) Dependence of pH on the peak current density ( $j_p$ ) on the negative-going scan. Blue and red dashed traces represent the molar fraction of  $\text{HCOOH}$  and  $\text{HCOO}^-$  in the solution. Solid curves are only a guide to the eye. Inset shows  $j_p$  examined in 0.1–1 M  $\text{HClO}_4$ . Owing to the weaker adsorption of  $\text{ClO}_4^-$ ,  $j_p$  is larger than in phosphate solutions. (c) Dependence of pH on the peak potential,  $E_p$ .

phosphate buffer solutions (or 0.1–1 M  $\text{H}_3\text{PO}_4$  and  $\text{HClO}_4$  for  $\text{pH} < 2$ ) containing 50 mM  $\text{HCOONa}$ . The rotating speed of the electrode employed here was 1000 rpm, but no significant effect of the rotation was observed, indicating that the reaction is controlled by kinetics. Since the voltammetric behavior on the positive-going scan is complex due to the co-adsorption of CO and to the surface oxidation of Pt, we focus on the oxidation peak on the negative-going scan that appears after the reduction of surface oxide, where the electrode surface is not significantly poisoned by  $\text{CO}_{\text{ads}}$ . The peak current of the oxidation peak,  $j_p$ , monotonically increases with increasing pH from 0 to  $\sim 4$  and then remarkably decreases at higher pHs (Figure 1b). Note that  $j_p$  is maximal at a pH close to the  $\text{pK}_a$  of  $\text{HCOOH}$ . The potential at which the oxidation current is maximal in the CVs,  $E_p$ , is also pH dependent and shifts to lower potentials with respect to the standard hydrogen electrode (SHE) at a rate of  $-60 \text{ mV}$  per pH unit (Figure 1c).

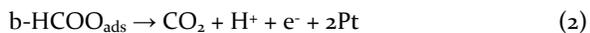
The increase of  $j_p$  with increasing pH in acidic and neutral media apparently cannot be explained by the direct  $\text{HCOOH}$  mechanism. The adsorbed formate mechanism is not compatible with the result either because the coverage of bridge-bonded formate, as probed by ATR-SEIRAS, decreases with pH and falls to zero at  $\text{pH} > 6$  (Supporting Information, Figure S1). Rather, the result suggests that  $\text{HCOO}^-$  is more reactive than  $\text{HCOOH}$  and that most of the current corresponds to its oxidation. However, if it is so, why does the oxidation current decrease at  $\text{pH} > 5$  despite the further increase of  $\text{HCOO}^-$  concentration (red dotted curve in Figure 1b)? John et al.<sup>15</sup> investigated the oxidation of  $\text{HCOO}^-$  in alkaline media and proposed that  $\text{HCOO}^-$  is adsorbed on the Pt electrode so strongly that its oxidation is very slow. However, the adsorbates detected by ATR-SEIRAS at  $\text{pH} > 6$  were  $\text{CO}_{\text{ads}}$ , water, and phosphate anions (most likely  $\text{HPO}_4^{2-}$  and  $\text{PO}_4^{3-}$ ), and no signals corresponding to the proposed strongly adsorbed  $\text{HCOO}^-$  or other related species were detected. Accordingly, it is reasonable to assume that  $\text{HCOO}^-$  is adsorbed only weakly and oxidized very quickly, and that its adsorption is significantly suppressed in alkaline media.

To explain the experimental results, we propose a simple model schematically illustrated in Figure 2. The blue curve represents the potential dependence of the reaction rate of  $\text{HCOO}^-$  oxidation  $k_{\text{ox}}$  (the Butler-Volmer rate law). Since the oxidation of  $\text{HCOO}^-$  does not take place on the oxidized Pt surface in alkaline media,<sup>15</sup> the oxidation current should exhibit a peak in the CV (red curve). Adsorption of OH species also can suppress  $\text{HCOO}^-$  oxidation by blocking active sites.<sup>6c,15,16</sup> Although the concentration of  $\text{HCOO}^-$  is a strong function of pH,  $k_{\text{ox}}$  is independent of pH, while the potential of oxidation of Pt surface or OH adsorption shifts negatively at a rate of  $-60 \text{ mV}$  per pH unit. As a result, the oxidation peak shifts negatively with pH at the same rate and the current decreases. The validity of this model is substantiated in the following by mathematical modeling of steady-state voltammograms.

It has been established experimentally that  $\text{HCOOH}$  is adsorbed on Pt as bridge-bonded formate (b- $\text{HCOO}_{\text{ads}}$ ) in acidic media:<sup>5,9,17</sup>



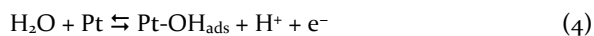
The missing of bridge-bonded formate at  $\text{pH} > 6$  is well correlated with the decrease of  $\text{HCOOH}$  concentration in the bulk, implying that bridge-bonded formate is formed only from  $\text{HCOOH}$ . Following Samjeské et al.,<sup>5</sup> bridge-bonded adsorbed formate is assumed to be irreversibly oxidized to  $\text{CO}_2$ :



Since the oxidation of  $\text{HCOO}^-$  via a weakly adsorbed  $\text{HCOO}^-$  precursor (direct  $\text{HCOO}^-$  pathway) is believed to be very fast, it is simply represented as



We will model the surface oxidation by a simple reversible reaction represented by



On a real polycrystalline surface,  $\text{OH}_{\text{ads}}$  is oxidized further to yield surface oxide.<sup>18</sup> However, to model the inhibition of  $\text{HCOOH}/\text{HCOO}^-$  oxidation by Pt surface oxidation, the introduction of  $\text{OH}_{\text{ads}}$  is sufficient in alkaline media,<sup>15</sup> and reaction 4 serves that purpose well. We do not consider the formation of  $\text{CO}_{\text{ads}}$  because  $\text{HCOOH}/\text{HCOO}^-$  is oxidized on a clean Pt surface not significantly poisoned by  $\text{CO}_{\text{ads}}$  on the negative-going scan. Adsorption of phosphate anions is also neglected for the sake of simplicity because a pH dependence of  $\text{HCOOH}/\text{HCOO}^-$  oxidation similar to that observed in phosphate buffered solutions (Figure 1) has also been observed in  $\text{ClO}_4^-$  and  $\text{HSO}_4^-/\text{SO}_4^{2-}$  solutions.<sup>14</sup>

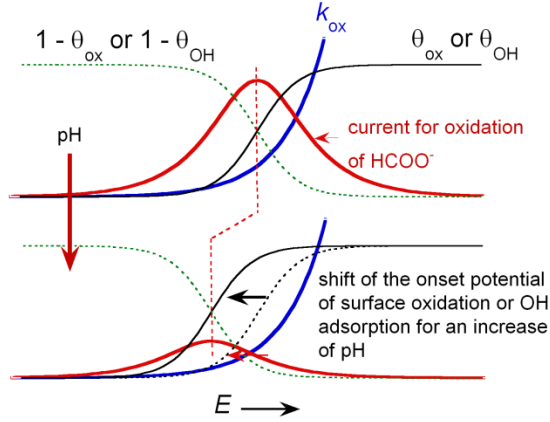


**Figure 2.** Schematic illustration of the negative shift of peak potential and of the decrease of peak current for an increase of pH.

Under these conditions, the coverage of bridge-bonded formate ( $\theta_{\text{b-f}}$ ) and adsorbed OH ( $\theta_{\text{OH}}$ ) satisfy the following differential equations:

$$\frac{d\theta_{\text{b-f}}}{dt} = k_1[\text{HCOOH}](1 - \theta_{\text{b-f}} - \theta_{\text{OH}}) - k_{-1}[\text{H}^+]\theta_{\text{b-f}} - k_2\theta_{\text{b-f}} \quad (5)$$

$$\frac{d\theta_{\text{OH}}}{dt} = k_4(1 - \theta_{\text{b-f}} - \theta_{\text{OH}}) - k_{-4}[\text{H}^+]\theta_{\text{OH}} \quad (6)$$

where  $k_i$  ( $i = \pm 1, 2, 3$ , and  $\pm 4$ ) is the rate constant of each reaction step at a potential  $E$  and is assumed to follow the Butler-Volmer rate law with a transfer coefficient  $\alpha$ :

$$k_i = k_i^{\text{eq}} \exp\left[\frac{\pm \alpha n F (E - E_i^{\text{eq}})}{RT}\right] \quad (7)$$

with plus for forward reaction (oxidation or adsorption) and minus for backward reaction (reduction or desorption).  $k_i^{\text{eq}}$  is the rate constant at the equilibrium potential  $E_i^{\text{eq}}$ , and  $F$ ,  $R$ , and  $T$  have the usual meanings. Although first order,<sup>7</sup> second order,<sup>6b,c</sup> and parabolic<sup>5</sup> rate equations with respect to  $\theta_{\text{b-f}}$  have been proposed for reaction (2), the first order rate law is assumed for the sake of simplicity. By applying the steady-state approximation

$$d\theta_{\text{b-f}}/dt = d\theta_{\text{OH}}/dt = 0 \quad (8)$$

the total current density  $j_{\text{total}}$  is given by adding up all contributions from the oxidation of  $\text{HCOOH}$  via bridge-bonded formate (reactions (1) and (2)),  $j_{\text{b-formate}}$ , and the direct  $\text{HCOO}^-$  oxidation (3),  $j_{\text{HCOO}^-}$ :

$$j_{\text{total}} = j_{\text{b-formate}} + j_{\text{HCOO}^-} \\ = 2Fk_2\theta_{\text{b-f}} + 2Fk_3(1 - \theta_{\text{b-f}} - \theta_{\text{OH}})[\text{HCOO}^-] \quad (9)$$

where

$$\theta_{\text{f}} = \left[1 + \frac{k_{-1}[\text{H}^+] + k_2}{k_1[\text{HCOOH}]} \left(1 + \frac{1}{K_4}\right)\right]^{-1} \quad (10)$$

$$\theta_{\text{ox}} = (1 - \theta_{\text{f}})/(1 + K_4) \quad (11)$$

and

$$K_4 = \frac{k_{-4}}{k_4}[\text{H}^+] = K_4^0[\text{H}^+] \exp\left\{\frac{-F(E - E_4^0)}{RT}\right\} \quad (12)$$

The steady-state voltammograms in Figure 3a, simulated by using parameters shown in the caption, show a significant pH dependence. The pH dependence of the total peak current  $j_{\text{total}}$ ,  $E_p$ , and  $\theta_{\text{b-f}}$  is in reasonable agreement with the experiment. The parameters related with bridge-bonded formate were chosen so as to trace the  $\text{HCOOH}$  concentration and  $E$  dependence of  $\theta_{\text{b-f}}$  reported in the literature.<sup>5d,7</sup> Other parameters were selected to fit the result in Figure 1. Among the parameters, the most important one is  $k_2^{\text{eq}}$ . It must be non-zero, i.e., bridge-bonded adsorbed formate is decomposed to yield  $\text{CO}_2$  although its contribution

( $j_{b\text{-formate}}$ ) to the total current is very small: Otherwise, the electrode surface would be fully covered by bridge-bonded formate in a wide  $E$  and pH range, and  $\text{HCOO}^-$  oxidation would be severely suppressed.

The most important finding in the simulation is that the current is predominantly carried by the oxidation of  $\text{HCOO}^-$  even in acid where its concentration is negligibly small (0.018% at pH 0). However, it can be supplied continuously from  $\text{HCOOH}$  through the acid-base equilibrium ( $\text{HCOOH} \rightleftharpoons \text{HCOO}^- + \text{H}^+$ ). On the other hand, the bridge-bonded formate pathway is much less active and suppresses the direct  $\text{HCOO}^-$  pathway by blocking active sites. However, the suppression of the direct  $\text{HCOO}^-$  pathway is not very significant despite the high  $\theta_{b\text{-f}}$  (Supporting Information, Figure S2) due to the positive shift of  $E_p$ . The dotted line in Figure 3b is the pH dependence of  $E_p$  when  $\theta_{b\text{-f}}$  is assumed to be zero. The positive shift of  $E_p$  by  $\sim 0.07$  V, caused by the adsorption of bridge-bonded formate, increases  $j_p$  by a factor of 4 (following the Butler-Volmer rate law). In the experiment, the shift amounts to  $\sim 0.2$  V in acidic and neutral media, which increases  $j_p$  by a factor of 49. Due to this effect, the experimental  $j_p$ - $E_p$  curve broadens into the low pH region, as can be seen from a comparison of Figures 1b and 3b.

Both the experiment and the simulation show that an optimal performance is obtained at a pH close to the  $\text{p}K_a$  of  $\text{HCOOH}$ . This is ascribed to the increase of  $\text{HCOO}^-$  concentration and to the decrease of the reaction rate with pH. The same trend has been observed also for the oxidation of some alcohols and aldehydes.<sup>14b</sup> If bridge-bonded formate is assumed not to be adsorbed on the electrode, as in the case of  $\text{HCOOH}$  oxidation on Pd,<sup>19</sup> the simulation showed that the maximum of  $j_p$  appears exactly at  $\text{pH} = \text{p}K_a$ . A theoretical thermodynamic argument has shown that this is a generic feature of decoupled proton-electron transfer reactions.<sup>20</sup> The same conclusion can be obtained also by using the simple kinetic model proposed in the present study (Supporting Information). Therefore, the  $\text{p}K_a$  of the molecule of interest is an important factor for predicting the optimal pH. In fact, electrocatalytic oxidation of alcohols that have large  $\text{p}K_a$  values is more facile in alkaline media than in acidic media.<sup>21</sup>

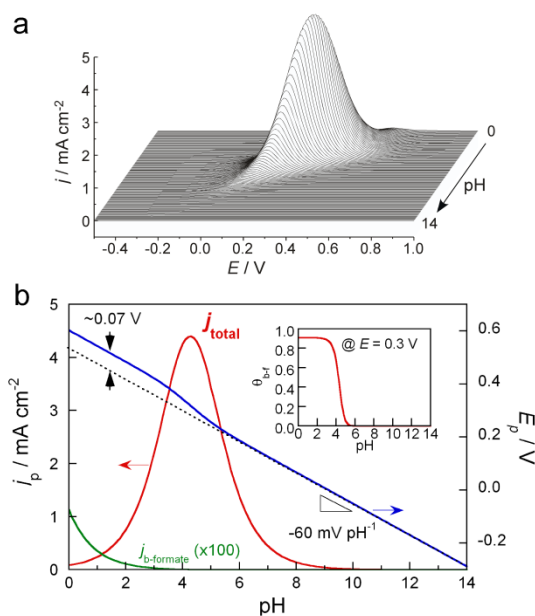


**Figure 3.** (a) Simulated pH dependence of the CV for  $\text{HCOOH}/\text{HCOO}^-$  oxidation. The parameters used were  $\text{p}K_a = 3.75$ ,  $[\text{HCOOH}/\text{HCOO}^-]_{\text{total}} = 50$  mM,  $\alpha = 0.5$ ,  $k_1^{\text{eq}} = 10^{-11}$  mol $^{-1}$  s $^{-1}$ ,  $k_{-1}^{\text{eq}} = 10^{-14}$  mol $^{-1}$  s $^{-1}$ ,  $k_2^{\text{eq}} = 10^{-15}$  s $^{-1}$ ,  $k_3^{\text{eq}} = 8 \times 10^{-9}$  s $^{-1}$ ,  $K_4^{\text{eq}} = 1$  mol $^{-1}$  s $^{-1}$ ,  $E_1^{\text{eq}} = E_2^{\text{eq}} = E_3^{\text{eq}} = 0$  V, and  $E_4^{\text{eq}} = 0.6$  V. (b) The simulated pH dependence of total peak current  $j_{\text{total}}$  (red curve) and that for the bridge-bonded formate pathway  $j_{b\text{-formate}}$  (green). Also shown is the pH dependence of the peak potential  $E_p$  (blue curve). The black dotted line is  $E_p$  neglecting the co-adsorption of bridge-bonded formate. Inset represents the pH dependence of the coverage of bridge-bonded adsorbed formate at 0.3 V.

A remaining issue is whether  $\text{HCOOH}$  is directly oxidized. Some theoretical simulations predict that the direct  $\text{HCOOH}$  oxidation is energetically much easier than the bridge-bonded adsorbed formate pathway.<sup>10,11</sup> However, we do not have any experimental evidence to support this mechanism at present. In addition, if it were the main reaction route in acidic media as Chen et al. argued<sup>9</sup> and the theoretical studies suggested,<sup>10,11</sup> a local minimum should appear in the  $j_p$ -pH plot in the pH range of 1-3 since the current carried by this mechanism should decrease monotonically as pH is increased, which conflicts with the experiment (figure 1). Furthermore, as has been discussed above, the oxidation of  $\text{HCOOH}$  through  $\text{HCOO}^-$  is very favorable. Therefore, the direct  $\text{HCOOH}$  mechanism is not likely to work.

So far, the mechanism of  $\text{HCOOH}$  oxidation has been discussed by focusing on the relationship between  $\theta_{b\text{-f}}$  and the oxidation current.<sup>5,6b,6c,7,9</sup> Note that the arguments have been made with an *a priori* assumption that the reactant is only  $\text{HCOOH}$ . However, as has been shown here, the major reactant is  $\text{HCOO}^-$  even in acidic media. Since the relationship between  $\theta_{b\text{-f}}$  and oxidation current is complex as has been discussed above and the weak adsorption of  $\text{HCOO}^-$  will be greatly affected by the co-adsorption of supporting anions, such arguments will not be fruitful. This is also the case in the theoretical studies in which the direct  $\text{HCOO}^-$  pathway was not taken into account.<sup>10-12</sup>

In summary, we have shown that  $\text{HCOO}^-$  is efficiently oxidized on Pt most probably via a weakly adsorbed  $\text{HCOO}^-$  precursor. Due to the low concentration of  $\text{HCOO}^-$  in acidic media and to the decrease of reaction rate in alkaline media, the oxidation

current reaches a maximum at a pH close to the  $pK_a$  of HCOOH. Oxidation of HCOOH takes place after it has been converted to  $HCOO^-$  through the acid-base equilibrium in the bulk near the electrode surface, as this pathway is more facile than its oxidation via bridge-bonded adsorbed formate and via a weakly adsorbed HCOOH precursor. The results reported in this Communication force to revise the interpretations made in earlier experimental and theoretical studies.

## ASSOCIATED CONTENT

### Supporting Information

Experimental details, SEIRA spectra of a Pt surface, kinetic analysis of a generic decoupled proton-electron transfer reaction, and suppression of oxidation current by bridge-bonded adsorbed formate. This material is available free of charge via the Internet at <http://pubs.acs.org>.

## AUTHOR INFORMATION

### Corresponding Author

osawam@cat.hokudai.ac.jp

### Author Contributions

These authors contributed equally.

### Notes

The authors declare no competing financial interests.

## ACKNOWLEDGMENT

This work was supported by Japanese Society for the Promotion of Science (JSPS) KAKENHI Grant Number 24550143 and 24750117 and MEXT Project of Integrated Research on Chemical Synthesis. MTMK gratefully acknowledges the award of Long-Term Fellowship of JSPS (No. L-11527) and Visiting Professorship of Hokkaido University. TU acknowledges Grants-in-Aid for Regional R&D Proposal-Based Program from Northern Advancement Center for Science & Technology of Hokkaido, Japan. JJ acknowledges scholarship of Asian Graduate School, Hokkaido University.

## REFERENCES

- (1) (a) Capon, A.; Parsons, R. *J. Electroanal. Chem.* **1973**, *44*, 1; (b) *J. Electroanal. Chem.* **1973**, *44*, 239; (c) *J. Electroanal. Chem.* **1973**, *45*, 205; (d) Parsons, R.; VanderNoot, T. *J. Electroanal. Chem.* **1988**, *257*, 9.
- (2) Jarvi, T. D.; Stuve, E. M. In *Electrocatalysis*; Lipkowsky, J., Ross, P. N., Eds.; Wiley-VCH: New York, 1998, p 75.
- (3) Sun, S.-G. In *Electrocatalysis*; Lipkowsky, J., Ross, P. N., Eds.; Wiley-VCH: New York, 1998, p 243.
- (4) Rees, N. V.; Compton, R. G. *J. Solid State Electrochem.* **2011**, *15*, 2095.
- (5) (a) Samjeské, G.; Osawa, M. *Angew. Chem. Int. Ed.* **2005**, *44*, 5694; (b) Samjeské, G.; Miki, A.; Ye, S.; Yamakata, A.; Mukouyama, Y.; Okamoto, H.; Osawa, M. *J. Phys. Chem. B* **2005**, *109*, 23509; (c) Samjeské, G.; Miki, A.; Ye, S.; Osawa, M. *J. Phys. Chem. B* **2006**, *110*, 16559; (d) Osawa, M.; Komatsu, K.; Samjeské, G.; Uchida, T.; Ikeshoji, T.; Cuesta, A.; Gutiérrez, C. *Angew. Chem. Int. Ed.* **2011**, *50*, 1159.
- (6) (a) Cuesta, A.; Cabello, G.; Gutiérrez, C.; Osawa, M. *Phys. Chem. Chem. Phys.* **2011**, *13*, 20091; (b) Cuesta, A.; Cabello, G.; Osawa, M.; Gutiérrez, C. *ACS Catalysis* **2012**, *2*, 728; (c) Cuesta, A.; Cabello, G.; Hartl, F. W.; Escudero-Escribano, M.; Vaz-Dominguez, C.; Kibler, L. A.; Osawa, M.; Gutiérrez, C. *Catalysis Today* **2013**, *202*, 79.
- (7) Grozovski, V.; Vidal-Iglesias, F. J.; Herrero, E.; Feliu, J. M. *ChemPhysChem* **2011**, *12*, 1641.
- (8) Osawa, M. *Bull. Chem. Soc. Jpn.* **1997**, *70*, 2861.
- (9) (a) Chen, Y. X.; Heinen, M.; Jusys, Z.; Behm, R. J. *Angew. Chem. Int. Ed.* **2006**, *45*, 981; (b) Chen, Y. X.; Heinen, M.; Jusys, Z.; Behm, R. J. *Langmuir* **2006**, *22*, 10399; (c) Xu, J.; Yuan, D. F.; Yang, F.; Mei, D.; Zhang, Z. B.; Chen, Y. X. *Phys. Chem. Chem. Phys.* **2013**, *15*, 4367.
- (10) Neurock, M.; Janik, M.; Wieckowski, A. *Faraday Discuss.* **2008**, *140*, 363.
- (11) Wang, H. F.; Liu, Z. P. *J. Phys. Chem. C* **2009**, *113*, 17502.
- (12) Gao, W.; Keith, J. A.; Anton, J.; Jacob, T. *J. Am. Chem. Soc.* **2010**, *132*, 18377.
- (13) Haynes, W. M. *CRC Handbook of Chemistry and Physics*; 92nd ed., 2011-2012.
- (14) (a) Buck, R. P.; Griffith, L. R. *J. Electrochem. Soc.* **1962**, *109*, 1005; (b) Bagotzky, V. S.; Vasiliev, Y. B. *Electrochim. Acta* **1964**, *9*, 869; (c) Adzic, R. R.; Hofman, M. I.; Drazic, D. M. *J. Electroanal. Chem.* **1980**, *110*, 361; (d) Kita, H.; Katagiri, T.; Kunimatsu, K. *J. Electroanal. Chem.* **1987**, *220*, 125; (e) Haan, J. L.; Masel, R. I. *Electrochim. Acta* **2009**, *54*, 4073.
- (15) John, J.; Wang, H. S.; Rus, E. D.; Abruna, H. D. *J. Phys. Chem. C* **2012**, *116*, 5810.
- (16) (a) Strasser, P.; Lubke, M.; Rempel, F.; Eiswirth, M.; Ertl, G. *J. Chem. Phys.* **1997**, *107*, 979; (b) Strasser, P.; Eiswirth, M.; Ertl, G. *J. Chem. Phys.* **1997**, *107*, 991.
- (17) Miki, A.; Ye, S.; Osawa, M. *Chem. Commun.* **2002**, 1500.
- (18) Angerstein-Kozłowska, H.; Conway, B. E.; Sharp, W. B. A. *J. Electroanal. Chem.* **1973**, *43*, 9.
- (19) Miyake, H.; Okada, T.; Samjeské, G.; Osawa, M. *Phys. Chem. Chem. Phys.* **2008**, *10*, 3662.
- (20) (a) Koper, M. T. M. *Phys. Chem. Chem. Phys.* **2013**, *15*, 1399; (b) Koper, M. T. M., *Chem. Sci.* **2013**, *4*, 2710.
- (21) Kwon, Y.; Lai, S. C. S.; Rodriguez, P.; Koper, M. T. M. *J. Am. Chem. Soc.* **2011**, *133*, 6914.

